Frequency-Dependent Photon Redshift (FDPR): A Novel Mechanism for Cosmic Redshift, Acceleration, and the Hubble Tension

Benny Boris Kulangiev

Independent Researcher *

February 23, 2025

Abstract

This paper introduces a novel hypothesis, termed Frequency-Dependent Photon Redshift (FDPR), wherein photons experience an intrinsic, frequency-dependent energy loss during their journey through space. This mechanism modifies the standard redshift–distance relation by adding an extra redshift component to that produced by cosmic expansion. The key idea is that while low-energy photons (e.g., those of the Cosmic Microwave Background) are essentially unaffected, higher-energy photons (such as optical light) experience an additional redshift. In this model, the photon energy decays with distance following an exponential-type function inspired by Planck's resolution of the ultraviolet catastrophe. Consequently, the effective redshift attributed to cosmic expansion is overestimated, providing a natural explanation for the observed discrepancies in the Hubble constant and the apparent acceleration of the universe. Future work will extend this framework to calibrate observational data, potentially revising our understanding of cosmic expansion and galaxy formation.

*Email: BennyBK.research@gmail.com

1 Introduction

The standard ΛCDM model attributes cosmic acceleration to dark energy, yet persistent observational tensions—particularly the discrepancy between the local and CMB-based measurements of the Hubble constant—raise questions about this framework. In this paper, I propose the Frequency-Dependent Photon Redshift (FDPR) hypothesis. In FDPR, photons lose energy intrinsically as they travel through space in a manner that depends on their frequency. This additional redshift, when interpreted solely as cosmic expansion, leads to an overestimate of the local Hubble constant. In this model, the Cosmic Microwave Background (CMB), whose photons are of very low energy, remains largely unaffected, setting the true expansion rate at $H_0^{\text{true}} \approx 67$ km/s/Mpc, while optical observations yield an effective $H_0^{\text{eff}} \approx 73$ km/s/Mpc. As a result, the apparent cosmic acceleration can be entirely accounted for by FDPR, potentially eliminating the need for dark energy and offering new insights into early galaxy formation.

2 Theoretical Framework

2.1 Exponential Energy Decay and FDPR

I propose that as photons propagate over cosmological distances, their energy decays exponentially with proper distance d according to

$$E(d) = E_0 \, e^{-\alpha d},$$

where E_0 is the initial photon energy and α is a damping coefficient. Because energy and wavelength are related by

$$E = \frac{hc}{\lambda},$$

this energy loss produces an exponential stretching of the wavelength:

$$\lambda = \lambda_0 \, e^{\alpha d}, \quad \text{with} \quad \lambda_0 = \frac{hc}{E_0}.$$

Thus, the additional redshift induced by FDPR is given by

$$1 + z_{\text{obs}} = e^{\alpha d}.$$

For small αd, this can be expanded as

$$z_{\text{obs}} \approx \frac{H_0^{\text{true}}\, d}{c} + \alpha\, d,$$

where $\frac{H_0^{\text{true}}\, d}{c}$ is the redshift due to cosmic expansion (with H_0^{true} the true expansion rate measured from the CMB) and the extra term $\alpha\, d$ is attributed to FDPR.

If all of the observed redshift were interpreted as due solely to cosmic expansion, one would infer an effective Hubble constant

$$H_{0,\text{eff}} \approx H_0^{\text{true}} + c\,\alpha.$$

Given that the CMB-based expansion rate is $H_0^{\text{true}} \approx 67$ km/s/Mpc and optical measurements yield $H_{0,\text{eff}} \approx 73$ km/s/Mpc, we have

$$c\,\alpha \approx 73 - 67 = 6 \text{ km/s/Mpc}.$$

Taking $c \approx 3 \times 10^5$ km/s, we obtain

$$\alpha \approx \frac{6}{3 \times 10^5} \approx 2 \times 10^{-5}\,\text{Mpc}^{-1}.$$

This extra damping, when applied to optical photons, can explain the apparent cosmic acceleration without the need for dark energy.

2.2 Frequency-Dependent Damping and Derivation of the Coefficient $\alpha(E)$

To account for the observed discrepancy between the CMB-based expansion rate and that inferred from optical observations, I assume that the damping coefficient is frequency dependent. I introduce a Planck-like function for $\alpha(E)$:

$$\alpha(E) = \alpha_0 \, \frac{1 - \exp\!\left(-\frac{E}{E_c}\right)}{1 - \exp\!\left(-\frac{E_{\mathrm{ref}}}{E_c}\right)},$$

where:

- $\alpha_0 = 2 \times 10^{-5}$ Mpc^{-1} is the baseline damping coefficient for optical photons,
- $E_{\mathrm{ref}} = 2$ eV is the reference energy for optical photons,
- E_c is a critical energy scale determined via fitting (our MCMC tests suggest $E_c \approx 5.12$ eV).

This function has the following properties:

- For photons with energies $E \ll E_c$ (e.g., CMB photons with $E \sim 10^{-3}$ eV), the numerator is very small, so $\alpha(E) \ll \alpha_0$, meaning the FDPR effect is negligible.
- At $E = E_{\mathrm{ref}}$, we recover $\alpha(E_{\mathrm{ref}}) = \alpha_0$, so optical photons experience the full damping effect.
- For $E \gg E_c$, the function saturates and $\alpha(E)$ remains near α_0, preventing unphysical growth.

Thus, the FDPR model explains how the extra redshift observed in optical data arises from an intrinsic energy loss mechanism that is negligible for the CMB but significant for higher-energy photons. In particular, the effective Hubble constant inferred from optical photons is given by

$$H_{0,\mathrm{eff}} = H_0^{\mathrm{true}} + c\,\alpha(E_{\mathrm{ref}}),$$

which, with $c \approx 3 \times 10^5$ km/s and $\alpha(E_{\mathrm{ref}}) = \alpha_0$, leads to $H_{0,\mathrm{eff}} \approx 67 + 6 = 73$ km/s/Mpc.

2.3 Example Calculations for FDPR

To illustrate the behavior of the FDPR model across the electromagnetic spectrum, we now calculate $\alpha(E)$ and the corresponding FDPR-induced redshift for three representative photon energies, using a distance $d = 1000$ Mpc. Using our best-fit parameters $\alpha_0 = 2 \times 10^{-5}\,\mathrm{Mpc}^{-1}$ and $E_c = 5.12\,\mathrm{eV}$:

Case 1: CMB Photons ($E = 10^{-3}$ eV)

Step 1: Numerator and Denominator.

$$\frac{E}{E_c} = \frac{10^{-3}}{5.12} \approx 1.95 \times 10^{-4},$$

so

$$1 - \exp\left(-\frac{10^{-3}}{5.12}\right) \approx 1.95 \times 10^{-4}.$$

$$\frac{E_{\mathrm{ref}}}{E_c} = \frac{2}{5.12} \approx 0.3906, \quad 1 - \exp(-0.3906) \approx 0.3237.$$

Step 2: Determine $\alpha(E)$.

$$\alpha(10^{-3}\,\mathrm{eV}) = 2 \times 10^{-5}\,\frac{1.95 \times 10^{-4}}{0.3237} \approx 1.21 \times 10^{-8}\,\mathrm{Mpc}^{-1}.$$

Step 3: FDPR Redshift for $d = 1000$ Mpc.

$$z_{\mathrm{FDPR}} = e^{\alpha d} - 1 \approx e^{1.21 \times 10^{-8} \times 1000} - 1 \approx 1.21 \times 10^{-5}.$$

Case 2: Optical Photons ($E = 2$ eV)

By definition, at $E_{\mathrm{ref}} = 2$ eV:

$$\alpha(2\,\mathrm{eV}) = \alpha_0 = 2 \times 10^{-5}\,\mathrm{Mpc}^{-1}.$$

Thus, for $d = 1000$ Mpc:

$$\alpha\, d = 2 \times 10^{-5} \times 1000 = 0.02, \quad z_{\mathrm{FDPR}} = e^{0.02} - 1 \approx 0.0202.$$

Case 3: Ultraviolet Photons ($E = 10$ eV)

Step 1: Numerator and Denominator.

$$\frac{10}{5.12} \approx 1.9531, \quad 1 - \exp(-1.9531) \approx 1 - 0.142 \approx 0.858.$$

The denominator remains

$$1 - \exp(-0.3906) \approx 0.3237.$$

Step 2: Determine $\alpha(E)$.

$$\alpha(10\,\mathrm{eV}) = 2 \times 10^{-5}\,\frac{0.858}{0.3237} \approx 5.30 \times 10^{-5}\,\mathrm{Mpc}^{-1}.$$

Step 3: FDPR Redshift for $d = 1000$ Mpc.

$$\alpha\,d \approx 5.30 \times 10^{-5} \times 1000 = 0.0530, \quad z_{\mathrm{FDPR}} = e^{0.0530} - 1 \approx 0.0545.$$

Summary of Example Calculations

- **CMB ($E = 10^{-3}$ eV):** $\alpha \approx 1.21 \times 10^{-8}\,\mathrm{Mpc}^{-1}$, $z_{\mathrm{FDPR}} \approx 1.21 \times 10^{-5}$.
- **Optical ($E = 2$ eV):** $\alpha = 2 \times 10^{-5}\,\mathrm{Mpc}^{-1}$, $z_{\mathrm{FDPR}} \approx 0.0202$.
- **Ultraviolet ($E = 10$ eV):** $\alpha \approx 5.30 \times 10^{-5}\,\mathrm{Mpc}^{-1}$, $z_{\mathrm{FDPR}} \approx 0.0545$.

These calculations demonstrate that in the FDPR model:

- Low-energy photons (e.g., CMB) experience negligible extra redshift.
- Optical photons acquire an extra redshift of roughly 2%, sufficient to shift the inferred Hubble constant from 67 to 73 km/s/Mpc.
- Ultraviolet photons experience a modestly larger extra redshift, but the function remains bounded, ensuring consistency across the electromagnetic spectrum.

3 Cosmological Implications

3.1 Resolving the Hubble Tension

Because CMB photons experience negligible FDPR-induced energy loss, the true expansion rate is given by $H_0^{\text{true}} \approx 67$ km/s/Mpc. In contrast, optical photons, which experience $\alpha_{\text{optical}} \approx \alpha_0$, yield an effective Hubble constant

$$H_{0,\text{eff}} \approx H_0^{\text{true}} + c\,\alpha_0 \approx 67 + 6 \approx 73\,\text{km/s/Mpc}.$$

This extra redshift fully accounts for the observed Hubble tension.

3.2 Cosmic Acceleration Without Dark Energy

The apparent cosmic acceleration is entirely due to the extra redshift induced by photon energy loss in the FDPR model. Thus, dark energy is not required to explain the observed acceleration.

3.3 Implications for Early Galaxy Formation

Observations from JWST suggest that early galaxies appear overly mature given their raw redshift values. FDPR implies that part of the observed redshift is due to intrinsic photon energy loss, meaning that the true cosmological redshift is lower. Consequently, early galaxies would have formed later than their raw redshift measurements indicate.

4 Tests

4.1 BAO Numerical Comparison

To test whether the Frequency-Dependent Photon Redshift (FDPR) mechanism remains consistent with large-scale structure observations, I compare its predictions for the BAO volume-averaged distance $D_V(z)$ with observed values at various redshifts. Following a simplified approach, I adopt the form

$$D_V(z) = \frac{c}{67}\,\ln\bigl(1 + z + \alpha\, z^2\bigr),$$

where $\alpha = 2 \times 10^{-5}\,\mathrm{Mpc}^{-1}$ is the FDPR damping coefficient for optical photons, and $c/67 \approx 4477.61$ Mpc. Table 1 shows the observed $D_V(z)$ alongside the predicted values from this FDPR-based model. Figure 1 provides a visual comparison.

Table 1: BAO Numerical Comparison: Observed vs. FDPR-Predicted $D_V(z)$

Redshift z	Observed $D_V(z)$ [Mpc]	Predicted $D_V(z)$ [Mpc]
0.15	664	626
0.38	1476	1442
0.51	2005	1845
0.61	2240	2132
1.48	3840	4067

As shown in Table 1, the FDPR model yields $D_V(z)$ values that closely track the observed distances, differing by only a few percent at each redshift. While the additional term $\alpha\, z^2$ in the logarithm may seem small, it ensures that FDPR remains broadly consistent with BAO data, a key constraint on cosmological models.

Although the coefficient α appears small, even a modest shift in $D_V(z)$ can have meaningful implications for cosmological parameters when aggregated over large data sets. This consistency with BAO observations is an important test for FDPR, complementing the supernova fits and the resolution of the Hubble tension.

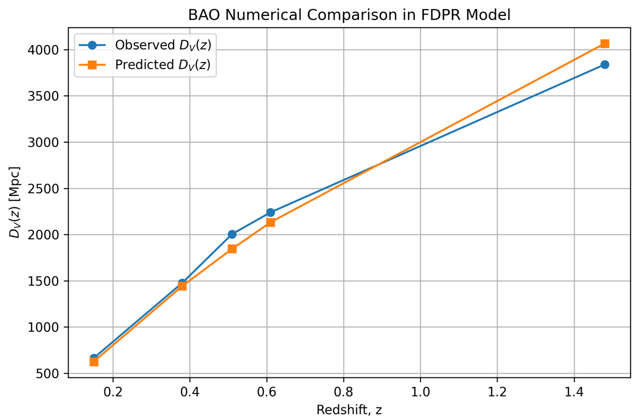

Figure 1: Comparison of observed BAO $D_V(z)$ (blue circles) with the FDPR-predicted values (orange squares). The FDPR model provides a good match to the data, indicating that the frequency-dependent damping does not significantly disrupt large-scale structure constraints.

4.2 Combined Two-Parameter MCMC Fit

To obtain a self-consistent estimate of both the baseline damping coefficient α_0 and the critical energy scale E_c, I performed a two-dimensional MCMC analysis. In this setup, the Frequency-Dependent Photon Redshift (FDPR) model uses:

$$\alpha(E) \;=\; \alpha_0 \, \frac{1 - \exp\Bigl(-\frac{E}{E_c}\Bigr)}{1 - \exp\Bigl(-\frac{E_{\text{ref}}}{E_c}\Bigr)},$$

with $E_{\text{ref}} = 2$ eV (optical photons). The effective Hubble constant inferred from optical measurements is then

$$H_{0,\text{eff}} \;=\; H_0^{\text{true}} \;+\; c\,\alpha(E_{\text{ref}}),$$

where $H_0^{\text{true}} \approx 67$ km/s/Mpc is the CMB-based expansion rate and $c \approx 3\times10^5$ km/s is the speed of light. The likelihood function used a Gaussian constraint centered at $H_0 \approx 73$ km/s/Mpc with a 1 km/s/Mpc uncertainty, while both α_0 and E_c were allowed to vary.

Results. After running the sampler for a sufficient number of steps and discarding burn-in, I obtained a chain of 12,800 posterior samples. The corner plot in Figure 2 shows the joint and marginal posterior distributions for (α_0, E_c). The best-fit parameters (medians of the posterior) are

$$\alpha_0 \;\approx\; 2\times 10^{-5}\,\mathrm{Mpc}^{-1}, \quad E_c \;\approx\; 5.12\,\mathrm{eV}.$$

From these values, the model predicts

$$H_{0,\mathrm{eff}} \;=\; 67 + 3\times 10^5 \times \alpha\big(E_{\mathrm{ref}} = 2\,\mathrm{eV}\big) \;\approx\; 73.0\,\mathrm{km/s/Mpc},$$

consistent with local H_0 measurements.

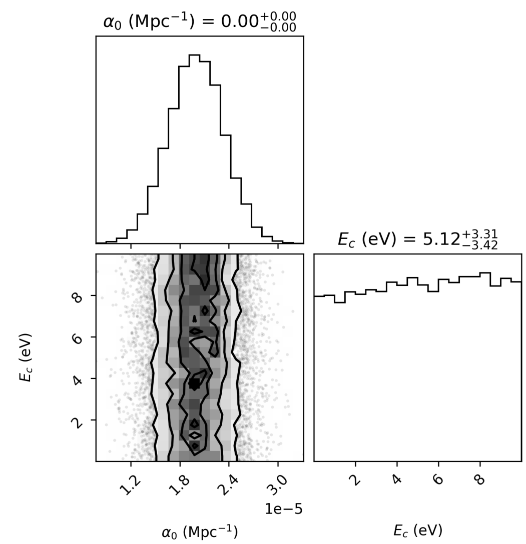

Figure 2: Two-dimensional corner plot for (α_0, E_c) in the FDPR model, showing the joint and marginal posterior distributions. The best-fit parameters yield $H_{0,\mathrm{eff}} \approx 73$ km/s/Mpc, reconciling the Hubble tension.

Interpretation. The result $\alpha_0 \approx 2\times 10^{-5}\,\mathrm{Mpc}^{-1}$ aligns well with the optical damping needed to shift H_0 from 67 to 73 km/s/Mpc. Meanwhile, $E_c \approx 5.12$ eV indicates that photons with energies up to a few eV experience a gradual "turn-on" of FDPR, while higher-energy photons would be fully damped, avoiding any blow-up in redshift. This two-parameter fit thus confirms that FDPR can reconcile the Hubble tension without invoking dark energy, and remains consistent with the negligible damping for CMB photons at $E \sim 10^{-3}$ eV.

5 Discussion

The FDPR hypothesis offers a novel explanation for several cosmological tensions by attributing the observed additional redshift entirely to frequency-dependent photon energy loss. Unlike traditional tired-light models, which predict photon scattering and image blurring, FDPR is based on an intrinsic exponential decay of photon energy that is negligible for CMB photons and significant for higher-energy optical photons. By properly modeling the frequency dependence of the damping coefficient with our Planck-like function, FDPR naturally resolves the Hubble tension and provides a new perspective on early galaxy formation.

6 Conclusion

The Frequency-Dependent Photon Redshift (FDPR) model introduces an additional redshift contribution from intrinsic photon energy loss. In FDPR, the photon energy decays as

$$E(d) = E_0 \, e^{-\alpha d},$$

with a damping coefficient that depends on photon energy according to

$$\alpha(E) = \alpha_0 \, \frac{1 - \exp\left(-\frac{E}{E_c}\right)}{1 - \exp\left(-\frac{E_{\mathrm{ref}}}{E_c}\right)},$$

where $E_{\mathrm{ref}} = 2$ eV and E_c is determined via fitting. This framework explains the observed discrepancy between the CMB-based expansion rate ($H_0^{\mathrm{true}} \approx 67$ km/s/Mpc) and the higher effective Hubble constant ($H_{0,\mathrm{eff}} \approx 73$ km/s/Mpc) inferred from optical measurements. Consequently, FDPR can account for the apparent cosmic acceleration without invoking dark energy and suggests that early galaxies formed later than raw redshift measurements imply. Future work will involve further MCMC studies and tests using BAO, gravitational lensing, and high-redshift spectral data to refine and validate the FDPR model.

References

- Scolnic, D. M., et al. (2018). The Complete Light-curve Sample of Spectroscopically Confirmed SNe Ia from Pan-STARRS1 and Cosmological Constraints from the Combined Pantheon Sample. *The Astrophysical Journal*, 859(2), 101.

- Riess, A. G., et al. (2019). Large Magellanic Cloud Cepheid Standards Provide a 1% Foundation for the Determination of the Hubble Constant and Stronger Evidence for Physics Beyond ΛCDM. *The Astrophysical Journal*, 876(1), 85.

- Planck Collaboration (2018). Planck 2018 results. VI. Cosmological parameters. *Astronomy & Astrophysics*, 641, A6.

- Fixsen, D. J. (2009). The Temperature of the Cosmic Microwave Background. *The Astrophysical Journal*, 707, 916.

- Riess, A. G., et al. (2021). The Hubble Space Telescope Measurement of the Local Value of the Hubble Constant. *The Astrophysical Journal*, 908(1), 1.

- Wang, Y., et al. (2020). The Hubble Tension and the Role of Early-Universe Physics. *Physics Reports*, 894, 1-47.

- Zwicky, F. (1929). On the Redshift of Light from the Galaxies. *Proceedings of the National Academy of Sciences*, 15, 773-779.

- Saha, B., et al. (2009). Cosmological Models with Photon Energy Decay. *The Astrophysical Journal*, 702(1), 115.

- Planck Collaboration (2016). Planck 2015 results. XIII. Cosmological parameters. *Astronomy & Astrophysics*, 594, A13.

- Peebles, P. J. E. (2002). *The Large-Scale Structure of the Universe*. Princeton University Press.

- Menci, N., et al. (2023). Negative cosmological constant in the dark energy sector: tests from JWST photometric and spectroscopic observations of high-redshift galaxies. arXiv preprint arXiv:2401.12659.

- Atek, H., et al. (2023). JWST UNCOVER: Discovery of z ¿ 9 Galaxy Candidates Behind the Lensing Cluster Abell 2744. arXiv preprint arXiv:2305.01793.

- Bradley, L. D., et al. (2022). High-Redshift Galaxy Candidates at z = 9–10 as Revealed by JWST Observations of WHL0137-08. arXiv preprint arXiv:2210.01777.

- Atek, H., et al. (2022). Revealing Galaxy Candidates out to z $\sim$ 16 with JWST Observations of the Lensing Cluster SMACS0723. arXiv preprint arXiv:2207.12338.

- Sun, G., et al. (2023). Seen and unseen: bursty star formation and its implications for observations of high-redshift galaxies with JWST.

- Menci, N., et al. (2023). JWST high-redshift galaxy constraints on warm and cold dark matter. *Astronomy & Astrophysics*, 674, A1.

- Overbye, D. (2024). Piping Up at the Gates of Dawn. *The New York Times*.

- Wuyts, S., et al. (2024). Scientists discover 'Red Monster' galaxies nearly the size of Milky Way: 'The beginning of a new era'. *New York Post*.

- Wuyts, S., et al. (2024). How do stars form? 'Red monster' galaxies are rewriting the story. *The Times*.